

# Sensitivity of a position sensitive detector with quadrant photodiode

Ž. Barbarić

State University of Novi Pazar, Serbia

## Email address:

[zbarbaric@np.ac.rs](mailto:zbarbaric@np.ac.rs) (Ž. Barbarić)

## To cite this article:

Ž. Barbarić. Sensitivity of a Position Sensitive Detector with Quadrant Photodiode. *Optics*. Vol. 2, No. 2, 2013, pp. 38-41.

doi: 10.11648/j.optics.20130202.12

**Abstract:** New relationships of displacement signal using four and only two opposite sectors on quadrant photodiode are derived. Sensitivity of position sensitive devices with quadrant photodiode is analyzed. The sensitivity is bigger for (1+1) than (2+2) configuration, for equal parameters. This is an important parameter in designing of command and control devices in laser guidance systems.

**Keywords:** A Position Sensitive Detector, Quadrant Photodiode, Displacement Signal, Sensitivity Of Device

## 1. Introduction

Lasers systems positioning have special treatment, because this resolution is bigger than radar and other devices. A number of application laser positioning includes tracking illuminated of target and its measurement of angular position [1], [2].

A precise determination of laser beam position or laser illuminated object position using quadrant photodiode can be made in two different arrangements of four photodiode sectors. In a combination, two and two sectors (2+2) are used [2], [3], in the second combination, only two sectors (1+1) are used [4] to obtained displacement signal. As it is known, a displacement signal is a function of the irradiance distribution on a sensitive surface of photodiode [2].

In this paper, a constant irradiance distribution is assumed since a derivation of displacement signal for the Gaussian distribution is too complicated. The relations of displacement signal and sensitivity of a position sensitive detector for both configurations (1+1) and (2+2) are derived. Sensitivity as a function of displacement distance is analysed.

## 2. Displacement Signals

Geometry of a quadrant photodiode with a laser spot centred at  $(x_0, y_0)$  is shown in Fig.1. Firstly, we assume a constant laser beam spot of radius  $r$ . Also, in Fig. 1, four segments and two coordinate systems are shown.

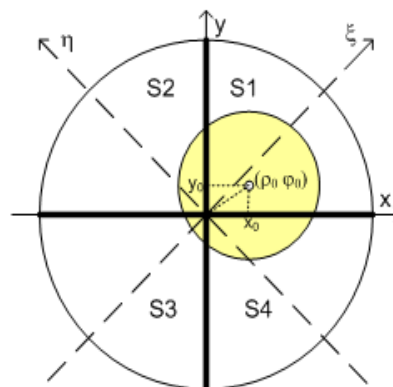


Fig.1. A quadrant photodiode geometry

A direct measurement of displacements  $x_0$  and  $y_0$  by processing signals from the quadrant photodiode is not possible. Having measured the signals, it is possible to determine the ratios of displacements and a light spot radius, e.g.  $x_0/r$  and  $y_0/r$ . For determining these relations, it is essential to know the irradiance distribution on the photodiode surface. The spot parameter in  $xoy$  coordinate system is given by the equation:

$$(x - x_0)^2 + (y - y_0)^2 = r^2 \quad (1)$$

The same equation in polar coordinates is obtained by the substitutions  $x = \rho \cos(\varphi)$ ,  $x_0 = \rho_0 \cos(\varphi_0)$  and  $y = \rho \sin(\varphi)$ ,  $y_0 = \rho_0 \sin(\varphi_0)$ , to obtain:

$$\rho^2 + \rho_0^2 - 2\rho\rho_0 \cos(\varphi - \varphi_0) = r^2 \quad (2)$$

If the irradiance on the photodiode surface is a constant one, then the optical power on sector is  $P_k = E_0 A_k$ , where  $E_0$  is the irradiance at the photodiode surface, and  $A_k$  is the area of the illuminated part of the  $k$ -th sector or quadrant of the photodiode.

The displacement signals along  $x$  and  $y$  axes are obtained from the difference of the signal received by the pair sectors. The difference of the signal power is a function of the irradiance, laser power and atmosphere conditions, and the distance between a laser source and photodiode. These are reasons for normalization form of displacement signals. A normalized form of displacement signal for combination of four sectors (2+2), we can write [2] for  $x,y$  orthogonal channels:

$$\begin{aligned} \varepsilon_x &= \frac{(A_1(\rho_0, \varphi_0) + A_4(\rho_0, \varphi_0)) - (A_2(\rho_0, \varphi_0) + A_3(\rho_0, \varphi_0))}{(A_1(\rho_0, \varphi_0) + A_4(\rho_0, \varphi_0)) + (A_2(\rho_0, \varphi_0) + A_3(\rho_0, \varphi_0))} \\ \varepsilon_y &= \frac{(A_1(\rho_0, \varphi_0) + A_2(\rho_0, \varphi_0)) - (A_3(\rho_0, \varphi_0) + A_4(\rho_0, \varphi_0))}{(A_1(\rho_0, \varphi_0) + A_2(\rho_0, \varphi_0)) + (A_3(\rho_0, \varphi_0) + A_4(\rho_0, \varphi_0))} \end{aligned} \quad (3)$$

The displacement signals along  $\zeta$  and  $\eta$  axes are obtained from the difference of the signal received by the sectors  $S_1$  and  $S_3$ , and  $S_2$  and  $S_4$ , respectively. A normalized form of displacement signals for two sectors (1+1), we can write [4] for  $\zeta,\eta$  orthogonal channels:

$$\begin{aligned} \varepsilon_\zeta(\rho_0, \varphi_0) &= \frac{A_1(\rho_0, \varphi_0) - A_3(\rho_0, \varphi_0)}{A_1(\rho_0, \varphi_0) + A_3(\rho_0, \varphi_0)} \\ \varepsilon_\eta(\rho_0, \varphi_0) &= \frac{A_2(\rho_0, \varphi_0) - A_4(\rho_0, \varphi_0)}{A_2(\rho_0, \varphi_0) + A_4(\rho_0, \varphi_0)} \end{aligned} \quad (4)$$

The displacement signals are assumed to be proportional to the areas along four quadrants, and they are calculated from the double integral being given here for the sector  $S_j$ :

$$A_j = \int_0^{\pi/2} \int_0^{\rho(\varphi)} \rho d\rho d\varphi = \int_0^{\pi/2} \frac{(\rho(\varphi))^2}{2} d\varphi \quad (5)$$

where  $A_j$  is the spot area on the first sector surface  $S_j$ .

The radius  $\rho(\varphi)$  is obtained from (2) in a form of

$$\rho(\varphi) = \rho_0 \cos(\varphi - \varphi_0) + \sqrt{(\rho_0 \cos(\varphi - \varphi_0))^2 - \rho_0^2 + r^2} \quad (6)$$

For sectors  $S_2, S_3$  and  $S_4$ , the limits of the angles  $\varphi$ , are respectively  $(\pi/2, \pi), (\pi, 3\pi/2), (3\pi/2, 2\pi)$ .

The normalized form of displacement signals in the combination (2+2), according to the Eq.(3), along  $x$  and  $y$  axes is obtained in the one

$$\begin{aligned} \varepsilon_x(\rho_0, \varphi_0) &= \frac{2}{\pi} \left( \frac{\rho_0}{r} \cos(\varphi_0) \sqrt{1 - \left(\frac{\rho_0}{r} \cos(\varphi_0)\right)^2} \right. \\ &\quad \left. + a \sin\left(\frac{\rho_0}{r} \cos(\varphi_0)\right) \right) \\ \varepsilon_y(\rho_0, \varphi_0) &= \frac{2}{\pi} \left( \frac{\rho_0}{r} \sin(\varphi_0) \sqrt{1 - \left(\frac{\rho_0}{r} \sin(\varphi_0)\right)^2} \right. \\ &\quad \left. + a \sin\left(\frac{\rho_0}{r} \sin(\varphi_0)\right) \right) \end{aligned} \quad (7)$$

The normalized form of displacement signals in the combination (1+1), according to the Eq.(4) along  $\zeta$  and  $\eta$  axes is obtained in the one

$$\begin{aligned} \varepsilon_\zeta(\nu_0, \varphi_0) &= \frac{\frac{\rho_0}{r} \cos(\varphi_0) \sqrt{1 - \left(\frac{\rho_0}{r} \cos(\varphi_0)\right)^2} + \frac{\rho_0}{r} \sin(\varphi_0) \sqrt{1 - \left(\frac{\rho_0}{r} \sin(\varphi_0)\right)^2} + a \sin\left(\frac{\rho_0}{r} \cos(\varphi_0)\right) + a \sin\left(\frac{\rho_0}{r} \sin(\varphi_0)\right)}{\frac{\pi}{2} + \frac{\rho_0^2}{r^2} \sin(2\varphi_0)} \\ \varepsilon_\eta(\nu_0, \varphi_0) &= \frac{\frac{\rho_0}{r} \sin(\varphi_0) \sqrt{1 - \left(\frac{\rho_0}{r} \sin(\varphi_0)\right)^2} - \frac{\rho_0}{r} \cos(\varphi_0) \sqrt{1 - \left(\frac{\rho_0}{r} \cos(\varphi_0)\right)^2} + a \sin\left(\frac{\rho_0}{r} \sin(\varphi_0)\right) - a \sin\left(\frac{\rho_0}{r} \cos(\varphi_0)\right)}{\frac{\pi}{2} - \frac{\rho_0^2}{r^2} \sin(2\varphi_0)} \end{aligned} \quad (8)$$

The normalized displacement signals (7) and (8) in polar coordinates are shown in Fig.2.

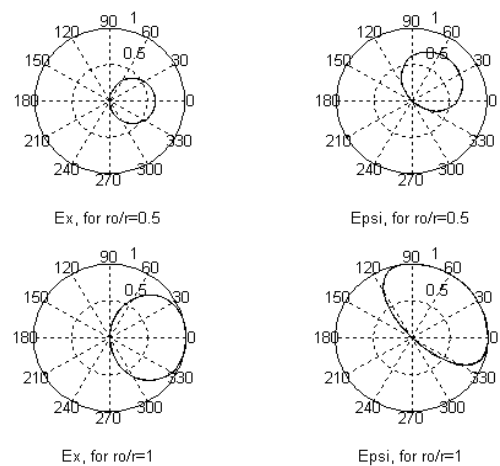


Fig. 2. The normalized displacement signals  $\varepsilon_x$  and  $\varepsilon_\zeta$  as a function  $\varphi_0$ , for  $\rho_0/r=0.5$  and 1.

The normalized displacement signals depend on both parameters, the maximum displacement signal is always around axes for each value of  $\rho_0/r$ , as it is shown in Fig.2.

Also, the normalized displacement signal increases with  $\rho_0/r$ , and the maximum value of displacement signal is obtained for  $\rho_0/r=1$ .

The normalized displacement signals (7) and (8) in the Cartesian coordinates are shown in Fig. 3.

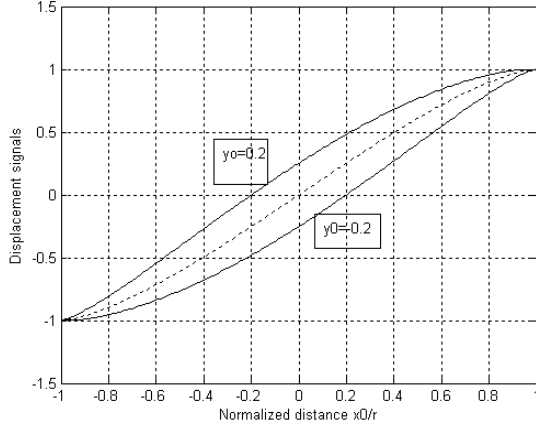


Fig.3. The normalized displacement signals  $\varepsilon_x$  (dotted) and  $\varepsilon_\zeta$  for two values of  $y_0/r$ , as a function of the normalized distance  $x_0/r$ .

The normalized displacement signal (7)  $\varepsilon_x$  (dotted) in Fig.3 is a function only to normalized displacement centres ( $x_0/r$ ). Therefore, the normalized displacement signal  $\varepsilon_\zeta$  from (8), for two sectors (1+1), is a function of both  $x_0/r$  and  $y_0/r$ ; as it is shown in Fig.3, for two values  $y_0/r$ . For other axes, the same result is obtained, as it is given in (7) and (8).

The normalized displacement signals  $\varepsilon_x$  and  $\varepsilon_y$  are dependent on only one coordinate, and can be used in an uncoupled laser tracking system. The normalized displacement signals  $\varepsilon_\zeta$  and  $\varepsilon_\eta$  are dependent on both coordinates, and can be used in a coupled laser tracking system.

### 3. Sensitivity

A sensitivity is defined as the first derivation of displacement signal. For (2+2) configuration, from (7), it is derived

$$\frac{\delta \varepsilon_x(\rho_0, \varphi_0)}{\delta \rho_0} = \frac{4}{\pi r} \cos(\varphi_0) \sqrt{1 - \left(\frac{\rho_0}{r} \cos(\varphi_0)\right)^2}$$

$$\frac{\delta \varepsilon_y(\rho_0, \varphi_0)}{\delta \rho_0} = \frac{4}{\pi r} \sin(\varphi_0) \sqrt{1 - \left(\frac{\rho_0}{r} \sin(\varphi_0)\right)^2} \quad (9)$$

From (9), the sensitivity tends to zero for  $\rho_0/r=1$ , and the sensitivity has the maximal value around the centre of photodiode, where  $S_{max}=4/(r\pi)$ ,  $\varphi_0=0$ . In Fig.4, the change of sensibility is shown as a function  $\rho_0/r$ .

The sensitivity is changeable in respect to  $\rho_0/r$  and  $\varphi_0$ , as it is shown in Fig.4. The maximum value of the sensitivity is around the centre quadrant photodiode,  $\rho_0=0$ . The sensitivity increases when the angle decreases, the angle is measured from  $x$ -axes.

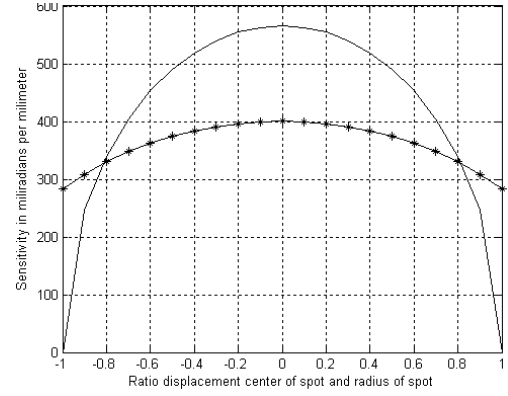


Fig.4. The sensitivity for (2+2) configuration as a function of normalized distance  $\rho_0/r$  ( $r=2.25\text{mm}$ ), for three values of  $\varphi_0=0$ , and  $\pi/4$  (\*\*).

Also, from (9), the sensitivity increases if the radius of spot decreases, for the constant  $\rho_0/r$ . In Fig. 5, the change of sensibility (9) as a function radius of spot is shown.

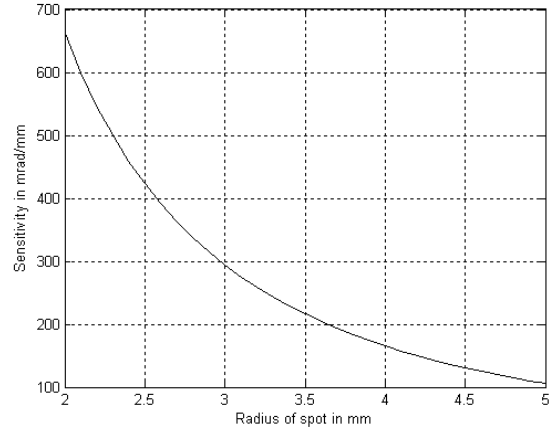


Fig.5. The sensitivity for (2+2) configuration as a function radius of spot  $\rho_0/r=0.5$  for  $\varphi_0=\pi/4$ .

A theoretical analysis of the quadrant photodiode sensitivity, where the Gaussian distribution of the light spot irradiance is assumed is given in [5]. The sensitivity was calculated for a full range of the ratio between the light spot radius and the photodiode radius. In this paper, it is shown that the sensitivity decrease, while the radius of spot increases.

The sensitivity for (1+1) configuration from (8) is derived for  $\varepsilon_\zeta$  displacement signal in the form of

$$\frac{\delta \varepsilon_\zeta(\rho_0, \varphi_0)}{\delta \rho_0} = \frac{2}{r} \frac{1 - 2\left(\frac{\rho_0}{r}\right)^2 \sin \varphi_0 \cos \varphi_0}{\frac{\pi}{2} + 2\left(\frac{\rho_0}{r}\right)^2 \sin \varphi_0 \cos \varphi_0} \left( \frac{\cos \varphi_0 \sqrt{1 - \left(\frac{\rho_0}{r}\right)^2 \cos^2 \varphi_0}}{+ \sin \varphi_0 \sqrt{1 - \left(\frac{\rho_0}{r}\right)^2 \sin^2 \varphi_0}} \right) \quad (10)$$

$$- \frac{4}{r} \frac{\left(\frac{\rho_0}{r}\right) \sin \varphi_0 \cos \varphi_0}{\frac{\pi}{2} + 2\left(\frac{\rho_0}{r}\right)^2 \sin \varphi_0 \cos \varphi_0} \left( \frac{a \sin((\rho_0/r) \cos \varphi_0)}{+ a \sin((\rho_0/r) \sin \varphi_0)} \right)$$

We can see the sensitivity (10) becomes too complicated

for the analysis. The change of sensitivity is given in Fig.6.

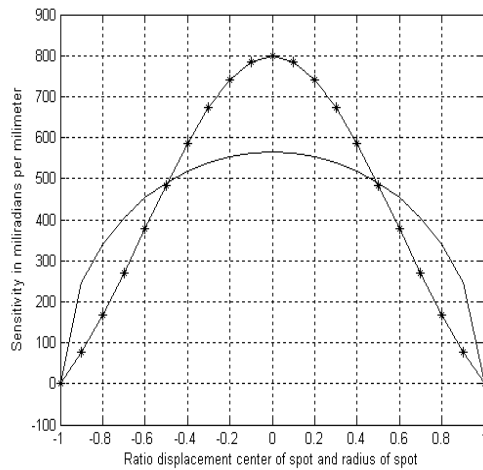


**Fig.6.** The sensitivity for (1+1) configuration as function of normalized distance  $\rho_0/r$  ( $r=2.25\text{mm}$ ), for two values  $\varphi_0=0$ , and  $\pi/4$  (\*\*).

The sensitivity is changeable in respect to  $\rho_0/r$  and  $\varphi_0$ , as it is shown in Fig.6. The maximum value of sensitivity is around the centre of quadrant photodiode,  $\rho_0=0$ . The sensitivity increases with the angle  $\varphi_0$ , the angle is measured from  $x$ -axes.

The sensitivity given in (9) and (10) for  $x$  and  $\zeta$  axes, as a function of angle  $\varphi_0$ , is shown in Fig.7.

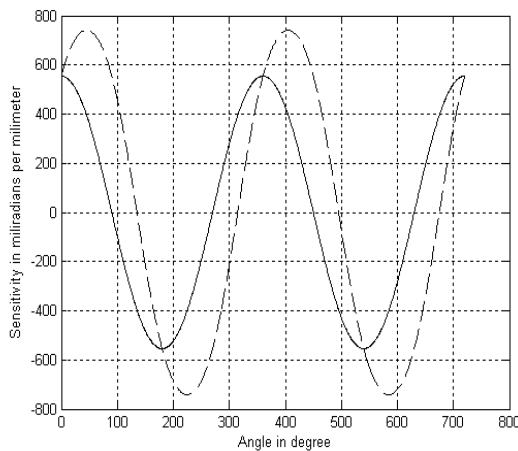


**Fig.7.** The sensitivity for (1+1,--), and (2+2) configurations as a function of angle  $\varphi_0$ , for  $\rho_0/r=0.2$ , and  $r=2.25\text{mm}$ .

The sensitivity for both configurations are changeable in respect to  $M$  as a  $\cos(\varphi_0)$ , as it is shown in Fig. 7.

The sensitivity is bigger for (1+1) than (2+2) configuration, for the equal parameters, as it is also seen, comparing

the diagrams in Fig.4 and Fig.6. The similar results are obtained in [6], only around the centre of the quadrant photodiode. This is a significant result in designing command and control devices of laser guidance systems.

## 4. Conclusion

The analysis of displacement signals shows that the normalized displacement signals  $\varepsilon_x$  and  $\varepsilon_y$  are independent, and can be used in the uncoupled laser tracking system, but the normalized displacement signals  $\varepsilon_\zeta$  and  $\varepsilon_\eta$  are dependent, and can be used in the coupled laser tracking system.

The analysis of the sensitivity where the constant distribution of the light spot irradiance is assumed. The sensitivity is calculated for the full range of the ratio between the distance centre of light spot and the light spot radius. The sensitivity in (1+1) configuration is better than the sensitivity in (2+2) configuration. This result can be used in designing command and control devices of the laser guidance systems.

## Acknowledgement

This paper has been partially supported by the Ministry of Science of Serbia under the Grant TR-32023.

## References

- [1] Mäkynen A, Kostamovaara J, Myllylä R., "Positioning Resolution of the Position-Sensitive Detectors in High Background Illumination", *IEEE Transactions on Instrumentation and Measurement*, 1996; 45: 324-326.
- [2] Ž. Barbarić, "Position Error of a Laser Illuminated Object", *Scientific Technical Review*, Vol. LII, No.5-6, Military Institute, Belgrade, 2002. pp. 25-30.
- [3] L. Manojlović, Ž. Barbarić, "Optimization of Optical Receiver Parameters for Pulsed Laser Tracking Systems", *IEEE Transactions of Instruments and Measurement*, Volume 58, Issue 3, 2009, pp. 681-690.
- [4] A. Marinčić, Ž. Barbarić, "Positioning signal analysis of novel quadrant photodiode arrangement", *Bulletin CXXXVIII de l'Academie serbe des sciences et des arts, Classe des sciences techniques*, No. 3, 2009, pp 80-85.
- [5] L. Manojlović, "Quadrant photodiode sensitivity", *APPLIED OPTICS*, Vol. 50, No. 20, 2011, pp. 3461-3469.
- [6] X. Hao, C. Kuang, Y. Ku, X. Liu, Y. Li, "A quadrant detector based laser alignment method with higher sensitivity", *ELSEVIER, Optik* 123, 2012, pp. 2238-2240.